

# Effect of Water-Soluble Polymers on the Morphology of Aerosol OT Vesicles

José I. Briz and M. Mercedes Velázquez<sup>1</sup>

Departamento de Química Física, Facultad de Ciencias Químicas, Universidad de Salamanca, Plaza de los Caídos s/n, 37008 Salamanca, Spain

Received May 30, 2001; accepted November 24, 2001

Vesicles of different morphologies were found to form in aqueous solutions of the surfactant sodium bis(2-ethylhexyl)sulfosuccinate, AOT, and in binary mixtures composed of AOT with poly(ethylene glycol) and poly(sodium 4-styrenesulfonate). Using electrical conductivity and fluorescence probing, two critical vesicle concentrations,  $c_{vc}$  and  $c_{ac}$ , were determined. These critical aggregation concentrations correspond to different kinds of aggregates, which are easily observed by optical microscopy. © 2002 Elsevier Science (USA)

**Key Words:** aerosol OT; vesicles; poly(ethylene glycol), poly(sodium 4-styrenesulfonate); electrical conductivity; fluorescence probing; video-enhanced optical microscopy.

Vesicles have attracted particular interest in the past years due to their applications in various scientific and applied fields (1). One major problem with these self-assembled structures is their insufficient stability. Nevertheless, this stability can be enhanced by the addition of oppositely charged amphiphiles (2–4) or single-tailed surfactant (5) or even hydrophilic polymers (6–12). The most studied systems contain mixtures of double-tailed and oppositely charged surfactants, while there is not enough information about the effect of polymers on the vesicle stability (6–8, 12). However, vesicle–polymer mixtures have recently attracted great interest as microreactors for polymerization reactions (9–11).

It is well known that the anionic surfactant sodium bis(2-ethylhexyl)sulfosuccinate (AOT) forms lamellar liquid-crystalline phase,  $L_{\alpha}$ , in water with a critical vesicle concentration (13),  $c_{vc}$ , of 6.1 mM at 29.9°C. With small-angle neutron scattering and X-ray experiments, the phase diagram of AOT/water mixtures has been obtained (12). Results have shown that the  $L_{\alpha}$  phase extends from  $C_{AOT} = 0.2$  and 0.7 ( $C_{AOT}$  is the surfactant weight fraction). In the  $C_{AOT}$  range between 0.014 and 0.2 the system is formed by  $L/L_{\alpha}$  in equilibrium. The phase separation takes place in mixtures with surfactant concentration below 0.08 after a few days, while above 0.08 no separation occurs. The observation of these solutions by means of optical polarized microscopy revealed the presence of spherulites.

Finally, mixtures containing surfactant concentration beyond 0.7 form cubic,  $Q_{\alpha}$ , and hexagonal,  $H_{\alpha}$ , phases. From these results one can conclude that even though the phase diagram of this system has been presented, the surfactant dilute region and vesicles region need to be clearly defined by obtaining the critical aggregation concentration of the different aggregates by means of techniques more sensitive to concentration than SANS, such as electrical conductivity, surface tension measurements (14), or fluorescence spectroscopy.

On the other hand, the effect of two water-soluble polymers, PAM (polyacrilamide,  $M_r = 5 \times 10^6$ ) and PEG (poly(ethylene glycol),  $M_r = 17,000$ ) on the AOT water phase diagram was also studied (12). No interaction was observed between PAM and the surfactant, while PEG stabilizes both dilute and concentrated lamellar phases. The phase separation occurs in the intermediate surfactant concentration range (12).

In the present work, we obtain the critical aggregation concentration of the different aggregation processes in the dilute surfactant concentration region,  $C_{AOT} < 0.16$ , in the absence and presence of two water-soluble polymers, PEG poly(ethylene glycol),  $M_r = 17,000$ ) and PSS (poly(sodium 4-styrenesulfonate),  $M_r = 75,000$ ). The aim of the present work is to study the effect of the addition of these polymers on the critical aggregation concentration of AOT and on the morphology of the AOT aggregates. The work is structured in two parts. In the first one a combination of electrical conductivity and fluorescence spectroscopy was used to obtain the critical aggregation concentration of the aggregates without and with polymers. In the second part, using the optical microscopy the morphology of the aggregates was observed.

## EXPERIMENTAL SECTION

**Materials and vesicle preparation.** Sodium bis(2-ethylhexyl)sulfosuccinate was purchased from Fluka. It was purified according to the published method (15). The surfactant showed no minimum in the surface tension–concentration plot (14), confirming its purity. Poly(ethylene glycol) ( $M_r = 17,000$ ) fraction was from Fluka and poly(sodium 4-styrenesulfonate), PSS ( $M_r = 75,000$ ) was from Aldrich. The molecular weights were provided by the manufactures. The fluorescence probe,

<sup>1</sup> To whom correspondence should be addressed. Fax: 00-34-923-294574. E-mail: mvsal@usal.es.

pyrene, was used as received from Aldrich. Sodium chloride, p.a. grade, was purchased from Panreac.

The pure vesicles are prepared by adding the calculated amount of surfactant to the solvent, water. The most dilute solutions are prepared by dilution from the stock concentrated solution. In polymer–surfactant mixtures the surfactant is dissolved in the polymer aqueous solution with a given concentration. In all cases care is taken not to use external energy input except a gentle stirring.

The solutions were prepared with water purified with RiOs and Milli-Q systems from Millipore and presented a conductivity of around  $0.2 \mu\text{S}/\text{cm}$ .

Incorporation of pyrene into vesicles was as follows: an appropriate volume solution of pyrene dissolved in methanol was poured into a volumetric flask and the solvent was evaporated. The solutions of surfactant or surfactant–polymer mixtures were added to the evaporated residue and the solution was stirred until the fluorescence probe was solubilized. The pyrene concentration was kept constant at  $1.5 \mu\text{M}$ .

Clear solutions for conductivity and fluorescence measurements were prepared,  $[\text{AOT}] < 0.03 \text{ M}$ , and except for electrical conductivity measurements where a titration method was employed, see below, solutions were prepared the day before and were maintained at  $30^\circ\text{C}$ . The micrographs of these solutions, see below, contain stable vesicles; therefore, this period of time was considered sufficient to obtain equilibrated structures.

**Conductivity measurements.** The electrical conductivity was measured with a conductometer model 727 from Metrohm operated at  $2.4 \text{ kHz}$ . A Metrohm Herisau conductivity cell, model AG 9101, was used. The cell constant,  $0.847 \text{ cm}^{-1}$ , was obtained by calibration with KCl solutions of known concentrations (16). Because the correct determination of the critical aggregation concentration by this method requires a large number of experimental data, a conductometric titration was employed in two ranges of AOT concentration. All measurements were done at  $30.0 \pm 0.1^\circ\text{C}$ . During the titration, solutions obtained by successive dilutions were allowed to equilibrate a few minutes until a stable measurement was obtained within the experimental error.

**Steady state fluorescence measurements.** The emission spectra of pyrene incorporated into AOT vesicles were recorded with the LS-50B spectrofluorometer. The excitation wavelength was  $319 \text{ nm}$  and the excitation and emission slits were kept constant at values of  $0.5/0.5$  or  $3/3 \text{ nm}$  as a function of the fluorescence intensity.

**Video-enhanced optical microscopy.** To obtain images of the samples, a video-enhanced optical microscope was used. This microscope consists of a light microscope Leika DMXRA model with a video camera mounted on top. The camera is connected to a video controller, which leads the video signal into a computer for image processing. Image analysis software can be used for digital enhancement and extraction of quantitative information.

## RESULTS AND DISCUSSION

**Conductivity measurements.** Electrical conductivity measurements have been widely used to obtain the cmc of pure or mixed ionic surfactant and are also used to evaluate the cvc of vesicle formation (5); therefore, they are used in this work to determine the critical aggregation concentration of these systems. Due to the width range of AOT concentrations studied in this work, we carried out the conductivity titration corresponding to concentrated and dilute surfactant regimes. Figure 1 collects some of these results. In all systems, two break points were detected in the slope of the conductivity surfactant concentration curves. The cac values determined from the intersection of the tangents drawn before and after the break point are in Table 1. The most dilute critical concentration of pure AOT agrees very well with the cvc found in the literature ascribed to AOT vesicle formation. The second critical concentration found in this work is  $19.7 \text{ mM}$ , named cac, could correspond to structural changes on the AOT vesicles or even to vesicles  $\leftrightarrow$  micelles transition.

The addition of PEG and PSS polymers to AOT aqueous solutions decreases both cvc and cac; see Table 1. This is a classical behavior in mixtures with polymer–surfactant interaction (17). The critical concentration values are practically independent of the nature of the polymer and on its concentration in the whole range of polymer concentration studied in this work.

On the other hand, it is well known that the addition of salts leads changes on the morphology of AOT vesicles (18, 19). When the salinity of the medium is small, spherulites predominate, while at NaCl concentrations higher than  $0.075 \text{ M}$  tubular vesicles appear (19). Taking into account that the PSS polymer has  $\text{Na}^+$  as a counterion, we also study the influence of the addition of NaCl on the properties of AOT vesicles. We kept the NaCl concentration at  $4.7 \times 10^{-3} \text{ M}$  because it is the concentration equivalent to the free  $\text{Na}^+$  left by  $1.3 \times 10^{-5} \text{ M}$  PSS.

Conductivity titration of solutions containing  $4.7 \times 10^{-3} \text{ M}$  NaCl was also carried out and the same behavior was observed. The cac's values from electrical conductivity are also presented in Table 1, differences with respect to the values found for AOT/PSS mixtures are detected. This fact indicates that the effect of PSS on the critical concentrations of AOT is not exclusively due to the addition of  $\text{Na}^+$  ions.

From conductivity results it is also possible to determine the degree of vesicle ionization and the standard Gibbs energy associated with the polymer–surfactant interaction. In pure micelles the ionization degree,  $\alpha$ , was determined from the ratio of the slopes of the conductivity/surfactant concentration plots above and below the cmc (20). In some mixed surfactant micelles (21) or polymer–surfactant solutions (22), three linear relations represent the conductivity curves; therefore, two ionization degrees are calculated. If  $S_1$ ,  $S_2$ , and  $S_3$  represent the conductivity slopes respectively before the cvc, between the cvc and cac and above the cac, the first ionization degree,  $\alpha_V$ , is calculated from the ratio  $S_2/S_1$ , and the second one from the ratio  $S_3/S_1$ . The values

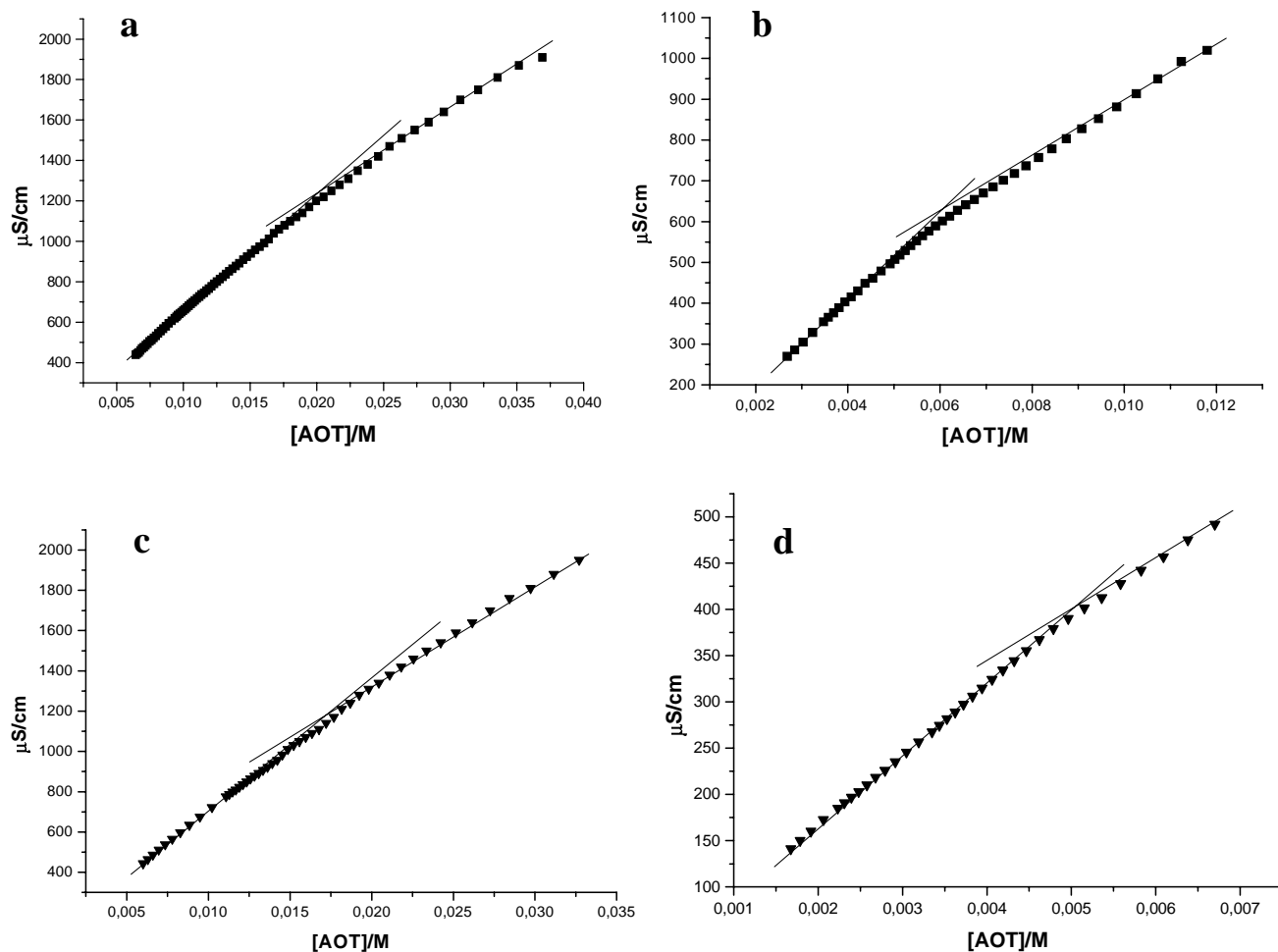


FIG. 1. Electrical conductivity of surfactant solutions: (a, b) AOT aqueous solutions and (c, d) mixtures composed of 0.05 mM PEG and AOT.

found in this work are listed in Table 2. In this table the ionization degrees of aggregates in saline solutions are also presented.

From the vesicle ionization degrees we conclude the following: (a) the degree of ionization found for vesicles without polymer was  $\alpha_V = 0.69$ . This value decreases for vesicles of AOT

concentrations greater than the  $cac$ ,  $\alpha_H$ . This fact indicates that these new aggregates have greater size (22) than the vesicles corresponding to a dilute surfactant concentration regime. (b) The degree of vesicle ionization,  $\alpha_V$ , increases when polymers are added and is not affected by the polymer nature or concentration.

TABLE 1

Critical Aggregation Concentration Values Obtained from Electrical Conductivity and Fluorescence Measurements

Additive	Electrical Conductivity		Fluorescence	
	cvc (mM)	cac (mM)	cvc (mM)	cac (mM)
0	7.8	19.7	7	Not detected
0.05 mM PEG	4.9	17.6		
0.12 mM PEG	3.5	18	6	Not detected
0.013 mM PSS	4.5	15		
0.016 mM PSS	4.4	17	4	10
4.7 mM NaCl	5.9	10.4	3	11.4

TABLE 2

Ionization Degree Values of AOT Vesicles Obtained from the Electrical Conductivity Measurements; Standard Gibbs Energy Values Found in This Work for the Transfer of AOT Monomers from Water to Vesicles

Additive	$\alpha_V$	$\alpha_H$	$\Delta G^\circ$ (kJ mol $^{-1}$ )
0	0.69	0.59	-15.9
0.05 mM PEG	0.79	0.66	-16.2
0.12 mM PEG	0.82	0.54	-16.8
0.013 mM PSS	0.85	0.71	-15.7
0.016 mM PSS	0.81	0.69	-16.2
4.7 mM NaCl	0.64	0.26	-17.6

(c) In systems containing polymers,  $\alpha_V > \alpha_H$ , indicating that the vesicles formed by concentrated AOT solutions have greater size than the dilute ones (22). (d) The degree of vesicle ionization in the AOT concentrated regime,  $\alpha_H$ , of NaCl aqueous solutions is lower than that of pure surfactant. This behavior has also been observed in micelles prepared in an excess of counterions and was explained as due to an increase of the charge neutralization at the Stern layer (23, 24). (e) Finally, the degrees of ionization of AOT/PSS and AOT/NaCl vesicles show significant differences. This is an additional argument that supports the hypothesis of the AOT-PSS interaction. This hypothesis will be confirmed from the images obtained by optical microscopy.

We have also calculated the standard free energy associated with the interaction between the surfactant and polymers,  $\Delta G^\circ$ , given by the standard Gibbs free energy of transfer of the surfactant monomer from the aqueous solution to the vesicle, which for monovalent counterions is (25)

$$\Delta G^\circ = RT(2 - \alpha_V) \ln c_{vc}. \quad [1]$$

The standard Gibbs energy calculated by Eq. [1] and the  $c_{vc}$  and ionization degrees values obtained by conductivity measurements are summarized in Table 2. The results show that the Gibbs energy is always negative since the vesicles are formed spontaneously. The Gibbs energy of transfer of the surfactant monomer from the aqueous solution to the vesicles is more negative in polymer solutions than in pure aqueous surfactant. From this fact we conclude that the addition of polymers stabilizes the vesicles. Nevertheless, there is not a great difference between the standard Gibbs energy without and with polymers; this seems to indicate a weak interaction between these polymers and the surfactant probably of hydrophobic origin (22). When the interaction is due to electrostatic origin, AOT mixed with NaCl, the interaction is stronger and the difference between the Gibbs energy in the absence and presence of NaCl increases; see Table 2.

Results from conductivity indicate the presence of two aggregation processes; one corresponds to the formation of AOT vesicles, while the origin of the second process cannot be determined by electrical conductivity measurements. This process could be due to monomer reorganization leading to aggregates of different morphology or to vesicles  $\leftrightarrow$  micelles transition. To study the origin of this critical concentration, fluorescence probing and video-enhanced optical microscopy were used.

*Steady state fluorescence measurements.* Fluorescence probing has been widely used to obtain critical micelle concentrations, cmc, of micelles and to estimate properties of the microenvironment of the probe in several kinds of micellar aggregates (26). The fluorescence experiments with pyrene as the probe are employed to evaluate the micropolarity of the hydrophobic core in micelles or the hydrocarbon bilayer in vesicles. The pyrene fluorescence fine structure presents five peaks. It is well established that the ratio between the intensities of the first (372 nm) and third (382 nm) vibration bands of the

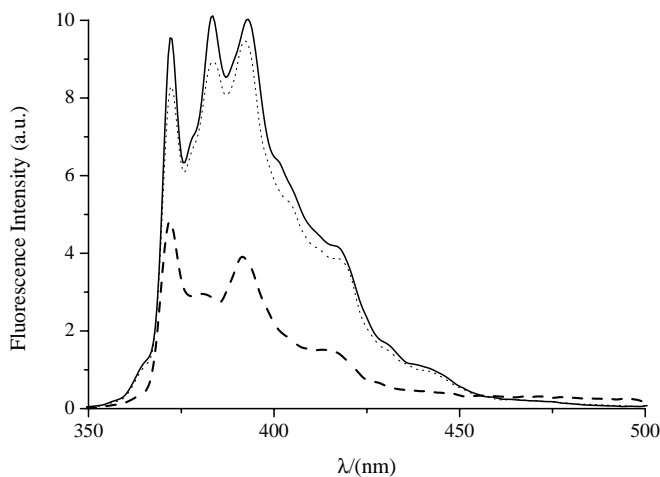
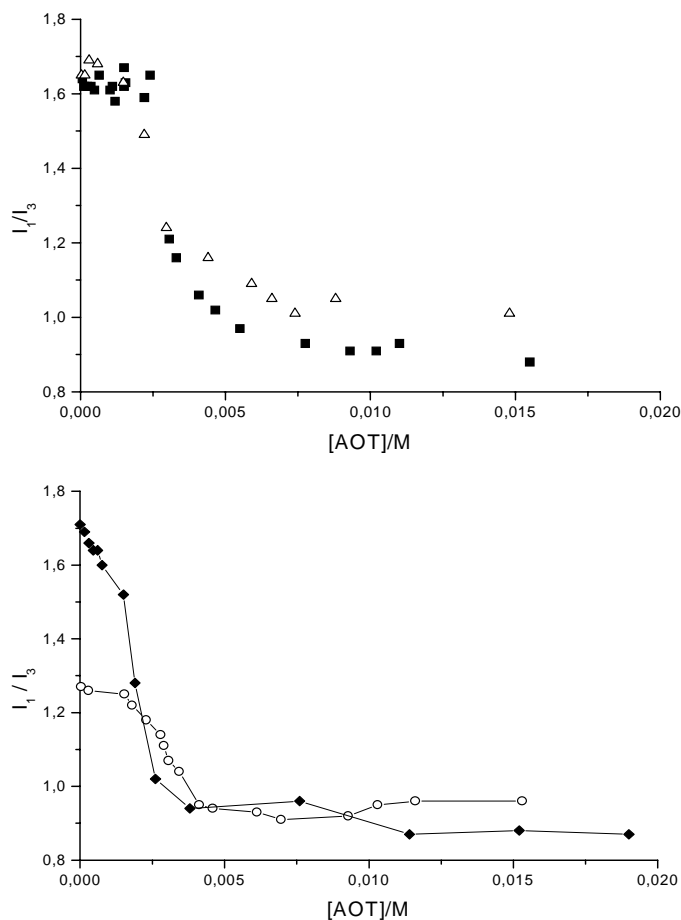


FIG. 2. Fluorescence spectra of pyrene solubilized in Aerosol OT aqueous solutions: dashed line,  $6.12 \times 10^{-4}$  M of surfactant; dotted line,  $1.55 \times 10^{-3}$  M; solid line, 0.011 M.

pyrene fluorescence spectrum,  $I_1/I_3$ , is related to the polarity of the pyrene environment (27). Low values of the  $I_1/I_3$  ratio correspond to a nonpolar environment. This ratio increases as the polarity of the medium rises (27). Since pyrene is solubilized inside the hydrocarbon chain of vesicles (28), the information obtained from fluorescence of pyrene in our systems refers to the bilayer of the vesicle (29). For orientative purposes the spectra of pyrene solubilized in surfactant solutions with different AOT concentrations are represented in Fig. 2.

Figure 3 presents the results for pure AOT and PEG-AOT, PSS-AOT, and NaCl-AOT mixtures. The plot of the ratio of the intensities of the pyrene emission spectrum against the surfactant concentration shows a typical profile. In pure AOT solutions at concentrations much lower than the  $c_{vc}$ , the 1:3 peak ratio has a value of 1.65, corresponding to an aqueous solution of pyrene (27). As the surfactant concentration increases, this ratio decreases, indicating that the probe passes to a more hydrophobic environment until a particular concentration is reached at which the ratio remains constant. In vesicles this concentration corresponds to the  $c_{vc}$ . When this methodology is used, the  $c_{vc}$  of aqueous AOT found in this work was 7 mM, in good agreement with the value found by electrical conductivity. The  $I_1/I_3$  value at the  $c_{vc}$  is 0.90. When one compares this value with those corresponding to vesicles of DDAB (9) or DDAC (30) ( $I_1/I_3 \approx 1.33$ ), it is observed that the environment of pyrene in AOT vesicles is more hydrophobic than that in these cationic vesicles.

When PEG is added, the profile of the curve is maintained (Fig. 3), but the  $c_{vc}$  appears at around 6 mM AOT. The  $I_1/I_3$  value at the  $c_{vc}$  was 1.03. This value is higher than that for pure AOT vesicles, showing a more hydrophilic pyrene microenvironment. This fact could be explained by the presence of the polymer PEG adsorbed inside the bilayer or by an increase in the curvature of the interface, which permits a greater water



**FIG. 3.** Variation of the ratio between the intensities of the first (372 nm) and third (382 nm) vibration bands of the pyrene fluorescence spectrum with the AOT concentration for (squares) AOT pure solutions, (open triangles) AOT and 0.12 mM PEG, (open circles) AOT and 0.016 mM PSS, and (diamonds) AOT and 5.6 mM NaCl. The lines are guides to the eye.

penetration in the bilayer. The  $I_1/I_3$  vs surfactant concentration curves of pure AOT and AOT/PEG mixtures present only one break point corresponding to the cvc.

In vesicles of AOT mixed with PSS at surfactant concentrations lower than the cvc, the  $I_1/I_3$  ratio remains constant at 1.25. This value is the same for pyrene dissolved in the PSS aqueous solution determined in this work. When the surfactant concentration increases, the 1 : 3 peak ratio decreases and passes through a minimum around 8 mM of AOT. The ratio of intensities in the minimum was 0.91. Before the minimum the ratio remains constant at 4 mM and then passes through the minimum and reaches a constant value at around 0.01 M of AOT ( $I_1/I_3 = 0.96$ ). These changes on the polarity on the pyrene environment take place in the AOT concentration range comprised between 4 and 10 mM. These values correspond to the cvc and cac values obtained from conductivity curves.

A comparison between fluorescence results of pyrene incorporated into AOT/PSS and AOT/NaCl vesicles show differences. Thus, even though two break points are detected in the

two mixtures, the cvc and cac values are weakly different. In addition the  $I_1/I_3$  values at the cvc and cac are also different (0.98 and 0.87 for AOT/PSS and AOT/NaCl, respectively). Finally, in curves with two break points, the intensity ratio when the second kind of aggregates are formed is lower than the values found in micelles (26). This fact seems to confirm that the cac cannot be ascribed to vesicles  $\leftrightarrow$  micelles transition.

From these results, it seems that conductivity is more sensitive than fluorescence probing for the determination of the critical concentrations; only one value is detected using fluorescence while two values are observed by conductivity measurements. This limitation probably results from the fact that the environments of the fluorescence probe, pyrene, is similar in the two kinds of aggregates. This fact seems to indicate that the second critical concentration, cac, could be ascribed to a new aggregate formed by the reorganization of the vesicle monomers. To confirm this assumption, we obtain the images of some of these solutions.

*Video-enhanced optical microscopy images.* Images of solutions containing  $9 \times 10^{-3}$  and  $3.3 \times 10^{-2}$  M AOT were observed. These surfactant concentrations correspond to solutions above the cvc and cac, respectively. Figure 4 shows these images. The micrograph of the solution containing a surfactant concentration around the cvc (Fig. 4a) shows the existence of a small number of big vesicles of around  $6 \mu\text{m}$ . These aggregates have certain mobility. This hydrodynamic flow could be due to concentration gradients of the surfactant, which are equivalent to chemical potential gradients operating as a force on the aggregates.

The solution of 0.033 M AOT is cloudy and its image is presented in Fig. 4b. As can be seen in the figure, vesicles of diameter around  $4 \mu\text{m}$  predominate.

Figure 5 presents the micrographs of solutions composed of  $1.2 \times 10^{-4}$  M PEG and the surfactant concentration of  $7.4 \times 10^{-3}$  and  $3.7 \times 10^{-2}$  M AOT, respectively. The figure shows that the most dilute solution (Figure 5a) contains vesicles with a high degree of polydispersity, while in the most concentrated one,  $[AOT] > \text{cac}$ , empty and polymer-filled vesicles (dark spheres) coexist (Fig. 5b). The most concentrated solution is also cloudy. It can be observed that the solubilization of PEG did not cause a considerable structural change for vesicles as one compares with pure AOT vesicles with similar surfactant concentration.

We have also obtained the images of solutions containing mixtures of PSS ( $1.6 \times 10^{-5}$  M) and AOT. In the systems with the AOT concentration greater than the cvc,  $9.97 \times 10^{-3}$  M, small aggregates practically indistinguishable by this technique were observed. However, the micrograph of solutions containing  $3.3 \times 10^{-2}$  M AOT,  $[AOT] > \text{cac}$  (Fig. 6), shows the existence of vesicles. As can be seen in the figure, the morphology and the size of polymer-surfactant vesicles are different from AOT vesicles with PEG. The presence of PSS seems to connect the aggregates. The greater size of PSS might interpret the difference (31).

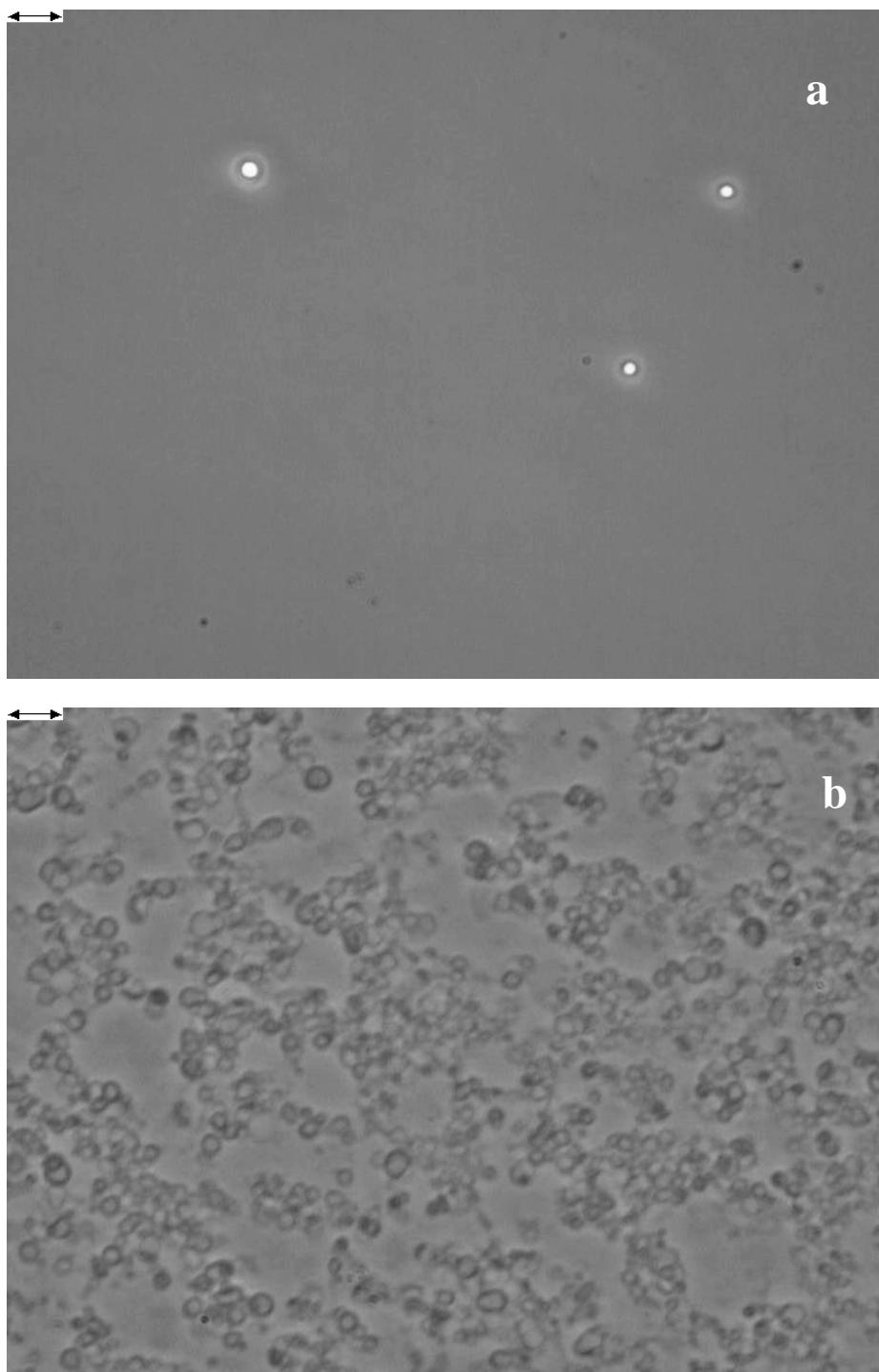
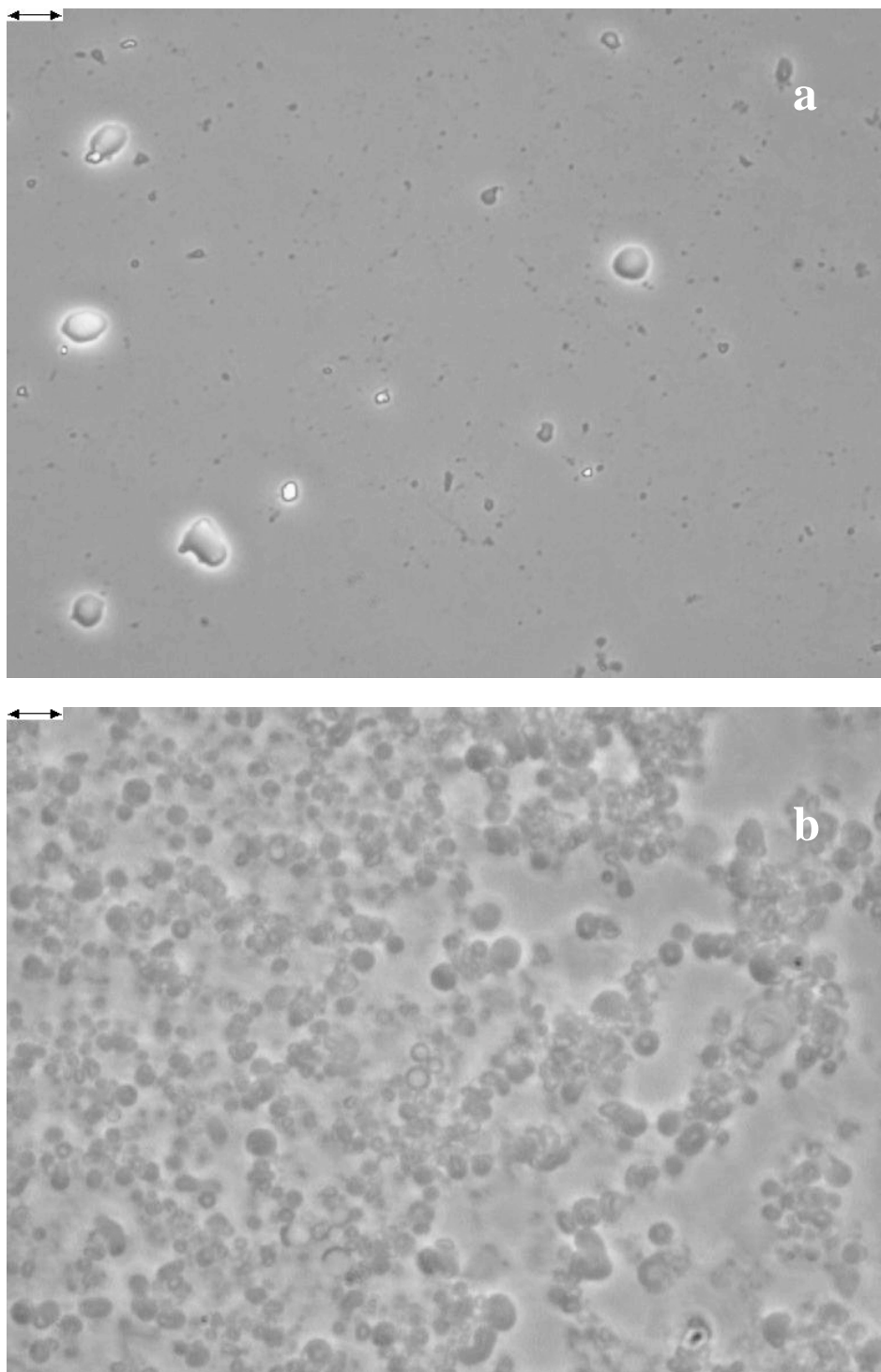


FIG. 4. Micrographs of fresh solutions containing (a)  $9 \times 10^{-3}$  M AOT and (b)  $3.3 \times 10^{-2}$  M of AOT. The scale bar corresponds to  $14 \mu\text{m}$ .

To compare the morphology of AOT-PSS with AOT-NaCl vesicles containing equivalent  $\text{Na}^+$  concentration, we have obtained the micrographs of mixtures with  $4.8 \times 10^{-3}$  M NaCl and different AOT concentrations. In the most dilute surfactant solutions,  $\text{AOT} \leq 0.014$  M, the size of aggregates is not great enough to be observed by optical microscopy. However, when the sur-

factant concentration increases,  $\text{AOT} = 0.028$  M, small vesicles are observed (Fig. 7). These aggregates are smaller than those formed in mixtures of PSS with similar AOT concentration.

The micrographs presented above correspond to solutions prepared the day before their observation with the microscope. We are also interested in observing the possible temporal



**FIG. 5.** Images obtained from video-enhanced optical microscopy of solutions containing  $1.2 \times 10^{-4}$  M PEG and the following AOT concentrations: (a)  $7.4 \times 10^{-3}$  M and (b)  $3.7 \times 10^{-2}$  M. The scale bar corresponds to  $14 \mu\text{m}$ .

evolution of these aggregates; therefore, we obtained the micrographs of these solutions 7 days after preparation. The results presented two different behaviors: The clear solutions  $[\text{AOT}] < 0.03$  M contain stable vesicles, while in the cloudy

solutions  $[\text{AOT}] > 0.03$  M the vesicle size is a metastable property. Figure 8 presents the images of these AOT-concentrated solutions. From Fig. 8a it can be seen that the AOT vesicles are transformed in tubular aggregates. In Figs. 8b and 8c are the

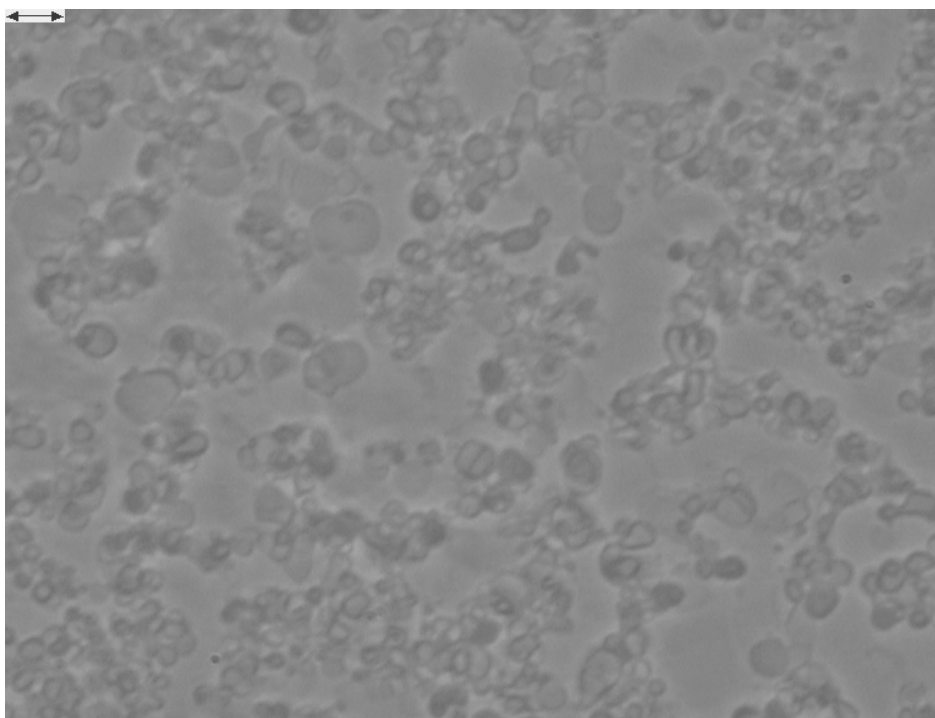


FIG. 6. Micrographs of fresh solutions composed of  $1.6 \times 10^{-5}$  M PSS with  $3.3 \times 10^{-2}$  M AOT. The scale bar corresponds to  $14 \mu\text{m}$ .

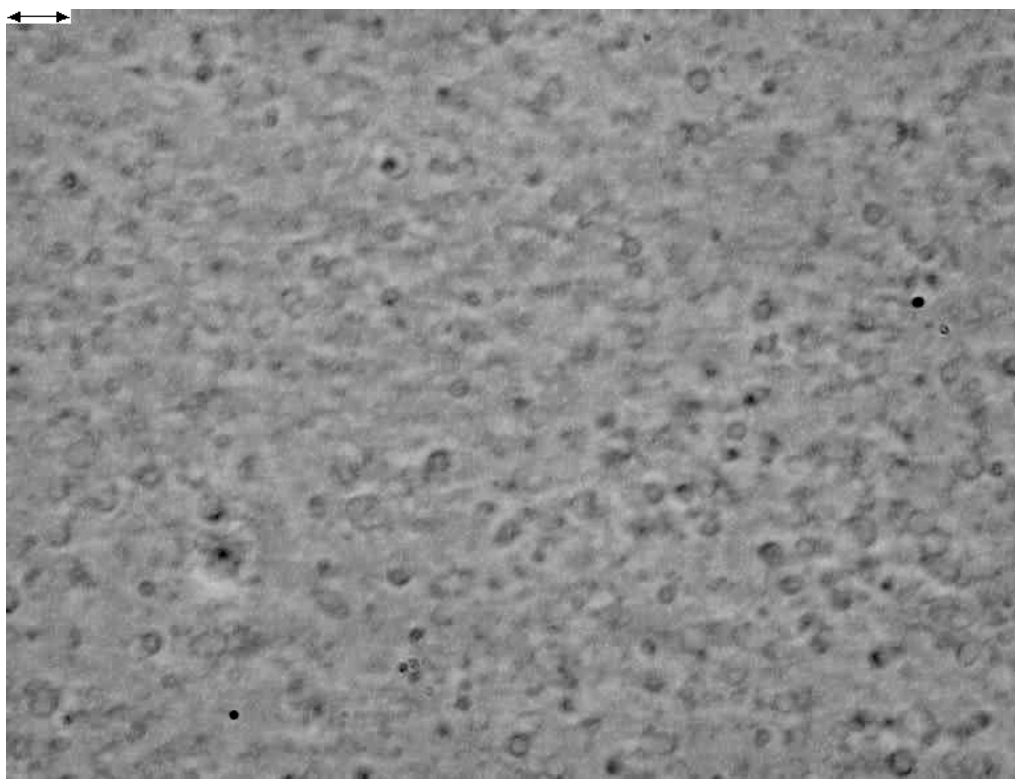
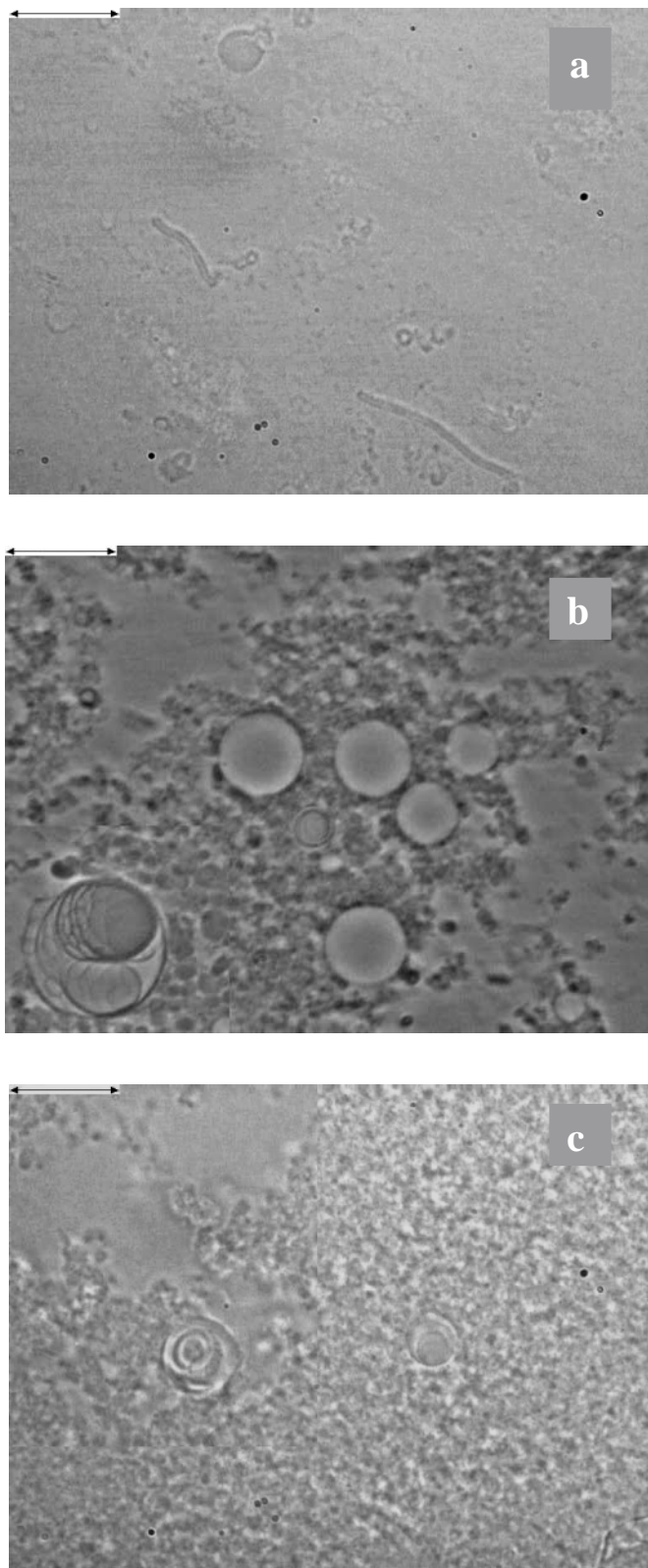


FIG. 7. Micrographs of fresh solutions composed of  $5.8 \times 10^{-3}$  M NaCl and 0.028 M AOT. The scale bar corresponds to  $14 \mu\text{m}$ .



**FIG. 8.** Images obtained 7 days after preparation of the following solutions: (a)  $3.3 \times 10^{-2}$  M AOT, (b)  $1.2 \times 10^{-4}$  M PEG and  $3.7 \times 10^{-2}$  M of AOT, and (c)  $1.6 \times 10^{-5}$  M PSS and  $3.3 \times 10^{-2}$  M AOT. The scale bar corresponds to 30  $\mu\text{m}$ .

micrographs of polymer–surfactant mixtures. The evolution of fresh vesicles is very different from that of pure AOT vesicles. In polymer–surfactant mixtures the small vesicles remain in the solution but at a lower percentage and big aggregates solubilized in a *tapestry* appear. All the *tapestry* moves with the same velocity. The movement is slow and the hydrodynamic flow cannot be explained by concentration gradients because all the *tapestry* moves with the same velocity. Since a new hydrophobic phase of polymer and surfactant molecules is created, a *chemically driven convection* (32) causes this flow. In this case the density gradient is developed between the water and the polymer–surfactant oil. This mechanism has been observed experimentally elsewhere (19, 33).

From the optical microscopy it seems that different kinds of lamellar aggregates appear depending on the AOT concentration and on the nature of the polymer. In addition, this technique confirms the existence of a second critical aggregation, named *cac*, ascribed to the formation of big vesicles. Finally, when the AOT concentration is greater than 0.03 M, the solutions became cloudy, and the vesicle structure is a metastable property.

## CONCLUSIONS

The results obtained in this work support the existence of vesicles in AOT aqueous solutions above the surfactant concentration of 7.8 mM, *cvc*. From electrical conductivity measurement a second critical concentration, *cac*, was determined. The *cvc* was also detected by fluorescence probing using pyrene as the probe. However, the electrical conductivity is more sensitive than fluorescence in determining critical concentration, and only in AOT/PSS and AOT/NaCl mixtures the *cac* was obtained by fluorescence.

The addition of PSS, PEG, and NaCl stabilizes the vesicles, decreasing both *cvc* and *cac*. The effect is independent of the kind of polymer and of its concentration. The *cvc* and *cac* of polymer–surfactant mixtures are  $(2.7 \pm 0.4) \times 10^{-3}$  and  $(13 \pm 1) \times 10^{-3}$  M, for AOT/PEG and AOT/PSS mixtures, respectively.

The morphology of aggregates formed at different surfactant concentrations and by the addition of the polymers is observed by video-enhanced optical microscopy.

## ACKNOWLEDGMENTS

The authors are most grateful to Dr. P. Pérez González from the Instituto de Microbiología Bioquímica, C.S.I.C./Universidad de Salamanca, for performing the optical microscopy experiments. This work is supported by Junta de Castilla y León and Fondo Social Europeo (Project SA04/99). The authors also acknowledge the Centro de Investigación y Desarrollo Tecnológico del Agua, C.I.D.T.A., for making available the fluorescence facility.

## REFERENCES

1. Lasic, D. D., “Liposomes: From Physics to Applications”. Elsevier, Amsterdam, 1993.

2. Kaler, E. W., Herrington, K. L., Murthy, A. K., and Zasadzinski, J. A. N., *J. Phys. Chem.* **96**, 6698 (1992).
3. Yacilla, M. T., Herrington, K. L., Brasher, L. L., Kaler, E. W., Chiuvalu, S., and Zasadzinski, J. A. N., *J. Phys. Chem.* **100**, 5874 (1996).
4. Caria, A., and Khan, A., *Langmuir* **12**, 6282 (1996).
5. Viseu, M. I., Velázquez, M. M., Campos, C. A., García-Mateos, I., and Costa, S. M. B., *Langmuir* **16**, 4882 (2000).
6. Raudino, A., and Castelli, F., *Macromolecules* **30**, 2495 (1997).
7. Ding, J., and Liu, G., *J. Phys. Chem. B* **102**, 6107 (1998).
8. Regev, O., Marques, E. F., and Khan, A., *Langmuir* **15**, 642 (1999).
9. Murtagh, J., and Thomas, J. K., *Faraday Discuss. Chem. Soc.* **81**, 127 (1986).
10. Meier, W., *Curr. Opin. Colloid Interface Sci.* **4**, 6 (1999) and references therein.
11. Poulain, N., Nakache, E., Pina, A., and Levesque, G., *J. Polym. Sci. Polym. Chem.* **34**, 729 (1996).
12. Ficheux, M. F., Bellocq, A. M., and Nallet, F., *Colloid Surf. A* **123–124**, 253 (1997).
13. Mukerjee, P., and Mysels, K. J., "Critical Micelle Concentration of Aqueous Surfactant Systems," National Standard Reference Data Series, p. 136. National Bureau of Standards (U.S.), Washington, DC, 1971.
14. Pedrosa, A. B., Briz, J. I., and Velázquez, M. M., submitted for publication.
15. Menger, F. M., and Yamada, K., *J. Am. Chem. Soc.* **101**, 6731 (1979).
16. Lind, J. E., Zwoleni, K. J. J., and Fuoss, R. M., *J. Am. Chem. Soc.* **81**, 1557 (1959).
17. Goddard, E. D., *Colloids Surf.* **19**, 255 (1986).
18. Ghosh, O., and Miller, C. A., *J. Phys. Chem.* **91**, 4528 (1988).
19. Shahidzadeh, N., Bonn, D., and Mennier, J., *Europhys. Lett.* **40**, 459 (1997).
20. Zana, R., Lianos, P., and Lang, J., *J. Phys. Chem.* **89**, 41 (1985).
21. Treiner, C., and Makayssi, A., *Langmuir* **8**, 794 (1992).
22. García-Mateos, I., Pérez, S., and Velázquez, M. M., *J. Colloid Interface Sci.* **194**, 356 (1997).
23. Phillips, J. N., *Trans. Faraday Soc.* **51**, 561 (1955).
24. Ford, W. P. J., Otterwill, R. H., and Parreira, H. C., *J. Colloid Interface Sci.* **21**, 522 (1966).
25. Hunter, R. J., "Foundation of Colloid Science, Vol. 1," p. 596. Oxford Univ. Press, Oxford, 1987.
26. Kalyanasundaram, K., "Photochemistry in Microheterogeneous Systems." Academic Press, Orlando, FL, 1987.
27. Kalyanasundaram, K., and Thomas, J. K., *J. Am. Chem. Soc.* **99**, 2039 (1977).
28. Ulmius, J., Lindman, B., Lindblom, G., and Drakenberg, T., *J. Colloid Interface Sci.* **65**, 88 (1978).
29. Vanderkooi, J. M., and Callis, J. B., *Biochemistry* **13**, 400 (1974).
30. Abuin, E., Lissi, E., Aravena, D., Zanocco, A., and Macuer, M., *J. Colloid Interface Sci.* **122**, 201 (1988).
31. Shioi, A., Harada, M., Obika, M., and Adachi, M., *Langmuir* **14**, 4737 (1998).
32. Bdzil, J. B., and Frisch, H. L., *J. Chem. Phys.* **72**, 1875 (1980).
33. Avnir, D. A., and Kagan, M., *Nature* **307**, 717 (1984).